MILLIMETRE WAVE RADAR SIGNATURES OF SEA LIONS

Samiur Rahman[1], Aleksanteri B Vattulainen[1], Duncan A Robertson[1], Ryan Milne[2]

[1]*School of Physics and Astronomy, University of St Andrews, North Haugh, St Andrews, Scotland*
[2]*Sea Mammal Research Unit, University of St Andrews, East Sands, St Andrews, Scotland*

Keywords: MILLIMETRE WAVE, RADAR, FMCW, SEA LION, MARINE AUTONOMY

Abstract

This study reports the millimetre wave radar signatures of sea lions collected from three animals in the outdoor seal pool available at the Sea Mammal Research Unit in St Andrews in the Autumn of 2021. The objective is to study the radar signatures of the animals when their full body or part thereof is above water. The data was collected using a 77 GHz Frequency Modulated Continuous Wave (FMCW) radar with linear polarisation. Both Horizontal-Horizontal (HH) and Vertical-Vertical (VV) polarisation data have been stored and analysed. It has been demonstrated that the sea lions were very clearly detected by the radar with SNR greater than 30 dB at a range of 40 m. The calculated radar cross section (RCS) of the sea lions in HH polarisation varies from -50 to -19 dBsm (modal) and -28 to -2 dBsm (maximum), corresponding to the different body parts and the amount of exposure to the radar beam. In VV polarisation, the modal RCS value range is from -47 to -25 dBsm and the maximum RCS varies from -26 to -15 dBsm. It is also shown that the recorded Doppler features have the potential for target classification, essential for autonomous operation of marine vessels.

1 Introduction

Due to the advancements in commercial millimetre wave chipset technology for the automotive industry, radars operating at these frequencies are now being explored for autonomous marine vessels. Radar plays a key role as a sensor due to its ability to work in practically all weather conditions. Traditionally, most marine navigation radars operate in X-band. In comparison, millimetre wave radars have the advantage of being compact and lightweight whilst simultaneously offering high resolution due to wide bandwidths and narrow beams. Such advantages means they can provide detailed information of the surroundings, as required for vessel autonomy

One of the main challenges for an autonomous marine vessel sensor is to detect and avoid large sized air breathing aquatic or semi-aquatic mammals (i.e. whales), which are protected species. To construct a reliable autonomous system, it is then very important to understand the radar signatures of such creatures in detail. This information can then be used for automatic target detection algorithm development. Currently, studies of the radar signatures of sea mammals are very scarcely reported in the literature. In [1], Results of humpback whales detected by X-band radar at ~8 km range in the Mediterranean sea were shown. Radar detection and tracking of fin whales and stenella dolphins up to 5.5 km at low sea states was also reported. In [2], detection of whales with an X-band Furuno radar mounted on NOAA R/V MacArthur II ship was reported. The radar obtained over 500 hours of data in moderate to high sea states [3]. The ship carried a census team who were used for visual observations. A total of 42 visual observations were made, which were used for radar data analysis. The radar target detection was done by simple Signal to Noise Ratio (SNR) thresholding. Various tracking algorithms were trialled, with no clear solution to overcome problems related to recurrent low SNR due to minimal exposure of the body (it was observed that the radar was not sensitive to whale spouts). A fully coherent and polarimetric X-band radar was used to obtain data of southern right whales in Australia [4]. This was a land based trial where the radar was positioned a t the edge of a cliff at Nullarbor Plain. The data collection was done over a wide range of incidence angles, so that the results can be applicable to ship-borne radars. Polarimetric domain analysis was performed on the collected radar data to enhance the contrast between the sea clutter and the target. In [5], another X-band radar (Kelvin Hughes) was deployed on the Isle of Eday, northern Scotland (for a different application), which detected Atlantic orcas. The results showed a pair of orcas undertaking surface activity and were detected and tracked at ~7 km range. The radar was incoherent, but was able to extract kinematic features for target classification. In [6], the presence of marine mammals in the Mediterranean sea were detected using an X-band radar.. A contiguous range-time-intensity plot based target classification algorithm was applied to the data, which was able to distinguish the observed 12 dolphins from other targets (ferries or sailing boats).

The aim of this study is to create a dataset of radar returns from different types of marine mammals at millimetre wave frequencies. The work is part of a wider project to assess the utility of sub-THz radars as sensors for marine autonomy, which requires knowledge of the radar signatures of objects on the sea surface, including sea mammals, which autonomous surface vessels would want to identify to make a manoeuvring decision. The trial corresponding to this study was the first campaign of the project, which will in future conduct further expeditions to gather marine mammal radar data. Along with the details of the experimental trial, this paper reports on the amplitude and Doppler properties of the measured data.

2. Experimental setup

Table 1 77 GHz radar (FAROS-E) parameters.

Parameter	Value
Centre frequency	76.5 GHz
Operating mode	FMCW
Tx power	25 dBm
Antenna beamwidth (one way)	13 ° (az. and el.)
Antenna gain	22.2 dBi
Polarisation	HH, VV
Bandwidth/range resolution	750 MHz/20 cm
Sampling rate	17.8125 MHz
Chirp time	114.97 µs
Chirp period	150.9 µs
Chirp Repetition Frequency (CRF)	6.63 kHz
Maximum unambiguous velocity	± 6.46 ms^{-1}

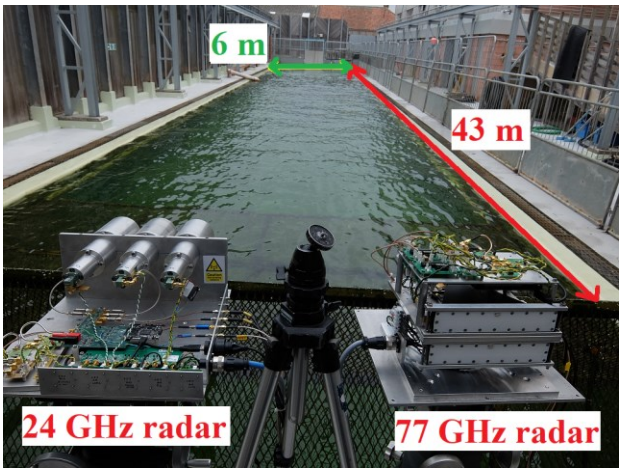

a

b

Fig. 1 (a) Pool used for experimental trial at the Sea Mammal Research Unit, St Andrews, (b) The three sea lions whose radar signatures were measured. .

The data collection proceeded on the 10th September, 2021 at the pool facility at the Sea Mammal Research Unit in St Andrews. Data were collected simultaneously with two radars operating at 24 GHz, named Blunderbuss [7] and 77 GHz, named FAROS-E [8]. This paper covers only the 77 GHz results.

The FAROS-E radar parameters are shown in Table 1. The radar was originally developed for real time drone detection, where a second version of that radar was developed for that application and this unit was modified for this particular field trial. This involved changing the antennas to wider beamwidth conical feedhorns to cover a wider arc length at short ranges. Additionally, the far field distance of the new antennas is quite small (~25 cm), appropriate for close range measurements. Waveguide straights were replaced by the waveguide twists to change the polarisation when needed. The anti-alias filter on the receive chain was set to suppress clutter beyond 40 m range, and the chirp parameters were adjusted to give a more suitable Doppler range. Radar calibration was performed a few days prior to the trial and confirmed the amplitude response was within 1-2 dB of theory.

As shown in Fig. 1 (a), the pool is 43 m long and 6 m wide. The radar was mounted on a tripod, 1.4 m above the ground, and pointed downwards by 5 ° along the long axis of the pool. The water and the ground were at the same level with negligible difference. The angle was optimised by carefully monitoring the clutter return coming from the surrounding metal bars at both sides and the end of the pool and selecting the region with the lowest clutter return whilst pointing along the pool. The antenna boresight was then pointing at the water's surface at approximately 16 m range. Despite this, strong static clutter backscatter could not be avoided completely due to the very confined measurement area. Moving Target Indication (MTI) filtering had to be used during signal processing to eliminate these clutter returns. All the radar measurements were performed in staring mode.

Three adult sea lions were present in the pool during the data collection period (Fig. 1 (b)). There was one male (length 2.1 m, weight 122 kg) and two females (length 1.8m, weight 80 kg). Radar data were collected for three different scenarios: i) opportunistic data collection whenever the sea lions were partially above water during their natural swimming, ii) dictating the sea lion movements in response to commands issued by their keeper (e.g. swimming with a flipper up) and iii) commanding the male sea lion to jump clear of the water towards a ball suspended above the pool.

3 Results

As seen in Fig. 2, the backscatter from the static clutter is very strong, in places greater than 60 dB above the radar noise floor of -93 dBm. It also shows no significant difference in the pool water backscatter between HH and VV polarisation. This masks any target return within the whole area of interest. To mitigate this, MTI processing was performed using the three-pulse canceller method [9]. It is an all-zero FIR filter with filter coefficients [1 -2 1]. The filtering was applied on the range processed complex data. Five consecutive chirps were used as

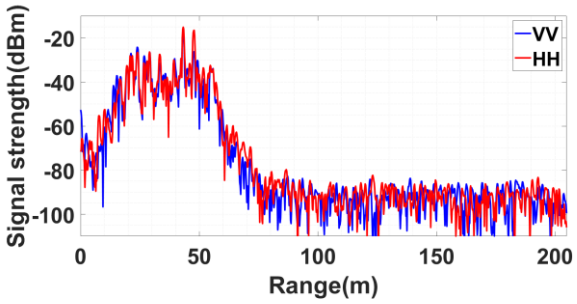

Fig. 2 77 GHz radar range profiles at HH and VV, showing very strong clutter returns from the pool up to ~60 m range.

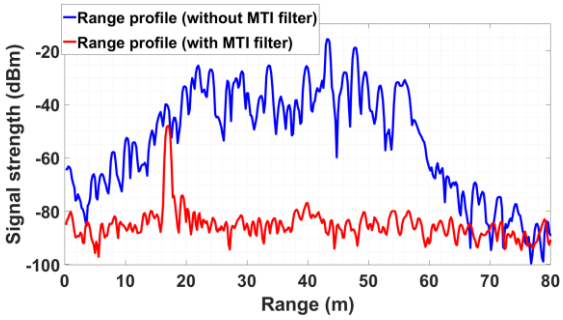

Fig. 3 Effect of MTI filtering for surrounding static clutter suppression. The return at 19 m is from a sea lion.

each slow time sequence during the filtering process, which gave very good results in terms of the static clutter removal from the datasets. Fig. 3 shows the effect of the MTI filter, where the presence of a target (one of the sea lions) is detected at 19 m range after applying the filtering, which was previously buried under the clutter return.

3.1 RCS calculation

To estimate the RCS of the sea lions, range-time-intensity plots are generated. An area of interest is at first selected from the range-time-intensity plot corresponding to a specific action of the sea lion, where in all cases the sea lion activity is observed from coincident video. Range bins occupied by the target are then selected by finding the signal peaks. The return signal strength values are later converted to RCS values using the radar calibration curve. The intensity plots also reveal the kinematic information of the animals. Antenna beam pattern information was also incorporated for RCS estimations, as quite often the targets were off the antenna boresight. A flattop window has been used for the amplitude data processing.

Fig. 4 (a) shows the range-time-intensity plot of an HH polarised dataset without MTI filtering. The strong clutter backscatter obscures virtually all target information. Different types of sea lion activity are clearly revealed after the MTI processing, as illustrated in Fig. 4 (b). The sea lions are detected with > 30 dB SNR in most cases. At ~4 s, the male sea lion jumped spontaneously, at ~30 m range, with the body almost orthogonal to the radar line of sight. The modal and maximum RCS values are calculated to be -19 and -2 dBsm respectively, seen in the histogram plot in Fig. 5(a). The

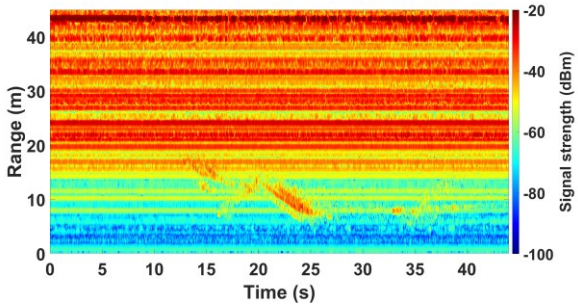

a

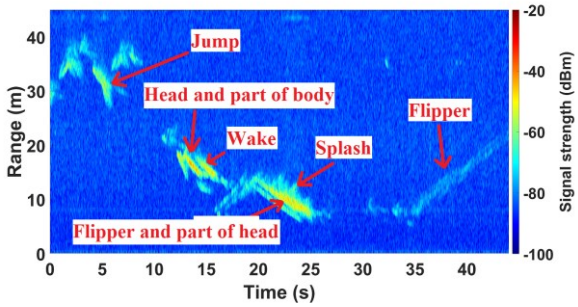

b

Fig. 4 (a) Range-time intensity plot of HH polarised data without MTI filtering, (b), and after MTI filtering, revealing sea lion activities.

second region at around 12-15 s is where two sea lions are coming towards the radar with roughly a quarter of their body above the water. The second one in Fig. 4(b) is selected as it has the highest return mainly due to being more visible to the radar. The third line is a breaking wave generated by the sea lion, showing that often the signatures of waves and the animals can be similar. The modal and maximum RCS calculated in this case are observed in Fig. 5 (b), which are -26 and -4 dBsm respectively. Between 20-25 s, they were swimming on their sides with one flipper above water, by command. One of them was also slapping it on the water, creating splashes, which can also be seen in Fig. 4 (b). The upper part of their body was also above water. Signal return only from this individual was traced as the other one was farther out of the antenna beam. The modal RCS is -34 dBsm and the maximum RCS is -12 dBsm, shown in Fig. 5 (c). From 35 s onwards, the diagonal lines in Fig. 4 (b) mostly correspond to the backscatter only from the flippers of the receding sea lions. Apart from the flipper, only a very small part of the head was also above water intermittently. Fig. 5(d) shows the corresponding histogram plot, where the modal and maximum RCS are found to be -50 and -28 dBsm respectively. Fig. 6(a) shows another range-time-intensity plot where two sea lions were slowly swimming towards the radar with their heads above the water, then disappearing after ~7 s. As the radar backscatter from the two targets is comparable here, a single histogram is generated with the return from both combined, which is illustrated in Fig. 6(b). The modal RCS

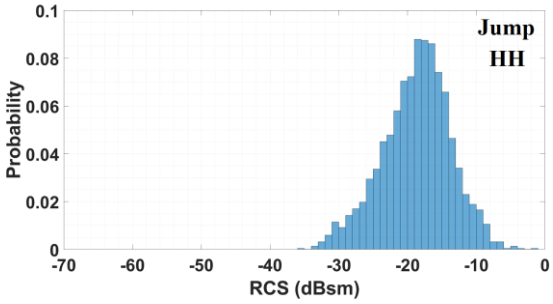

a

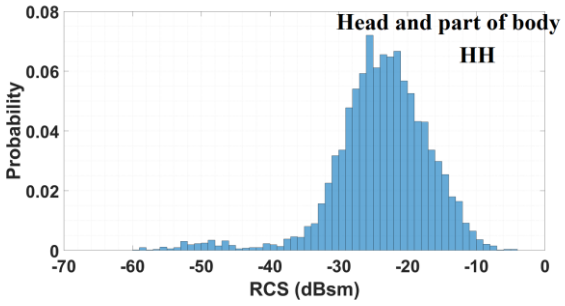

b

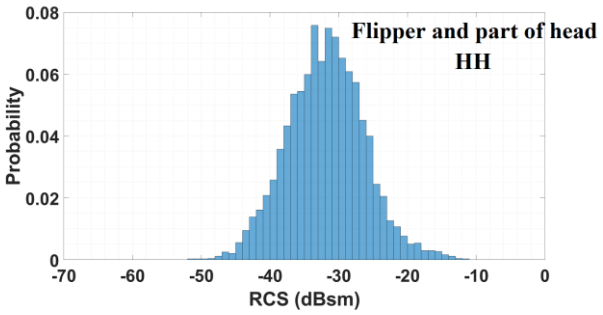

c

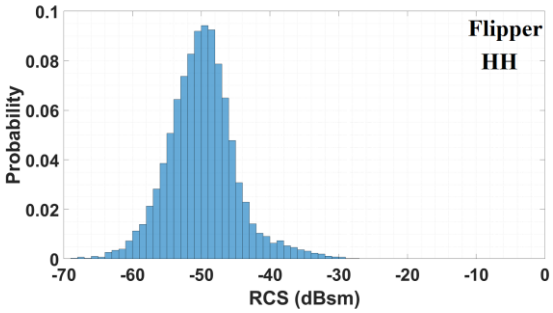

d

Fig. 5 HH RCS histograms of (a) sea lion, (b) sea lion head and part of body, (c) sea lion flipper and part of head, (d) sea lion flipper.

value is -48 dBsm and the maximum RCS is -20 dBsm. The

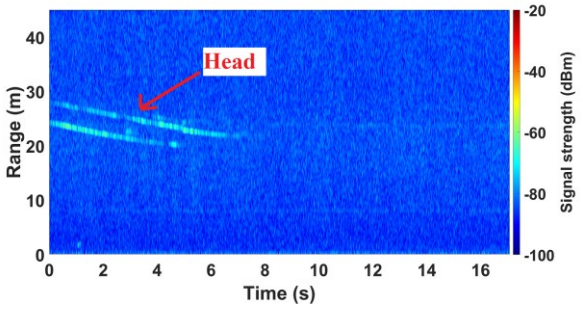

a

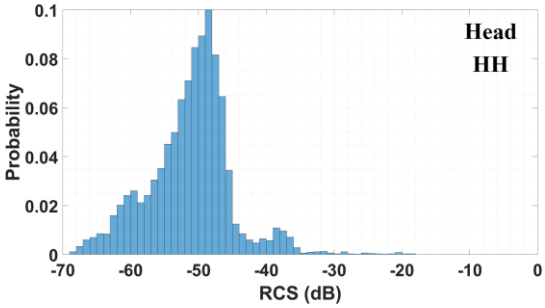

b

Fig. 6 (a) HH range-time intensity plot of two sea lion heads, (b) corresponding HH RCS histogram..

modal RCS might be lower here as sometimes their heads were usually submerged. .

Fig. 7 is a range-time-intensity plot processed for VV polarised data after MTI filtering. In the first ~7 s, two sea lions were approaching the radar with just their heads above the water. The RCS histogram plot for this period is shown in Fig. 8 (a), where the modal and maximum RCS values are -40 and -20 dBsm respectively. The maximum RCS is the same for the equivalent activity in HH, but the modal value is 8 dB higher. As mentioned before, this might be due to the occasional lack of body exposed above water in Fig. 6 (a), which can also be the reason for the comparatively broader RCS distribution in Fig. 8 (a). In Fig. 8 (b), an RCS histogram is plotted corresponding to a quick spontaneous jump of a sea lion at ~14 s. The modal RCS value

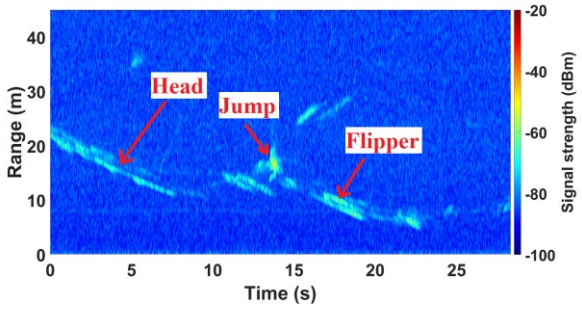

Fig. 7 Range-time intensity plot of VV polarised data.

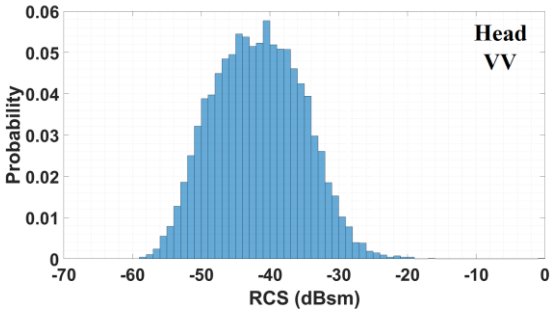

a

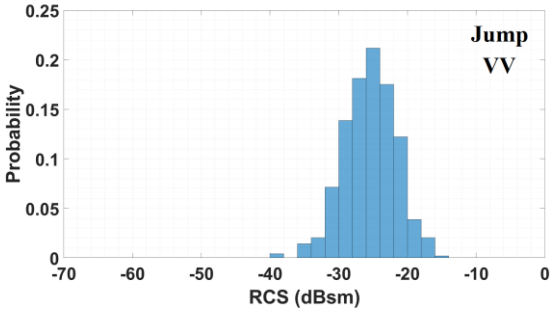

b

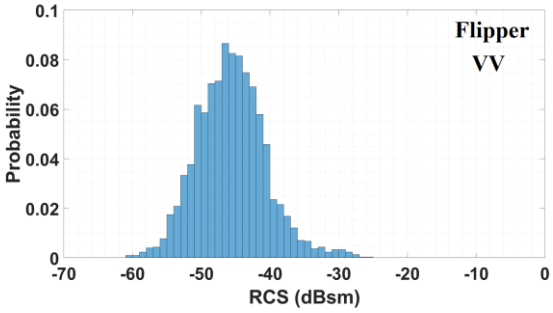

c

Fig. 8 VV RCS histograms of (a) sea lion head, (b) sea lion jumping, (c) sea lion flipper.

is -25 dBsm and the maximum RCS is -15 dBsm. These are quite low compared to the previous HH data, but may be due the fact that in this case the whole body was aligned more along the radar beam compared to the jump in Fig. 4 (b). From around 16-19.5 s in Fig. 7, two sea lions were approaching the radar with their flippers above the water along with a part of their upper bodies. The corresponding RCS values are -47 dBsm (modal) and -26 dBsm (maximum), seen in Fig. 8 (c). These are a few dBs higher than the corresponding movement in HH, but in this case the video file shows that perhaps slightly more body was exposed in the VV data, which might explain the slightly higher RCS.

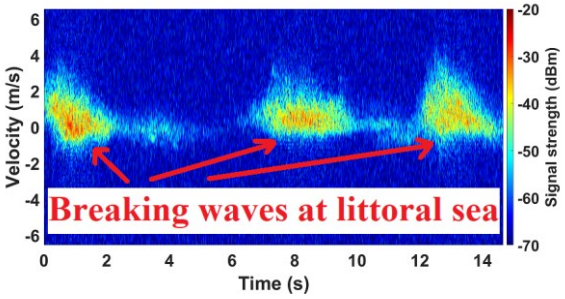

Fig. 9 94 GHz Doppler spectrogram of receding breaking waves at littoral sea.

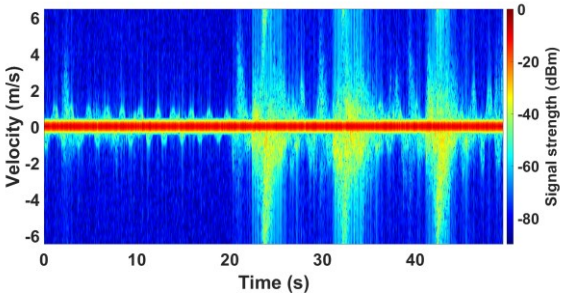

a

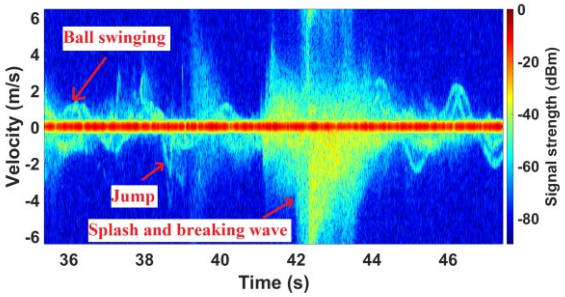

b

Fig. 10 (a) Doppler spectrogram plot of a sea lion jumping clear of the water, (b) Zoomed in version of the event.

3.2 Doppler analysis

Doppler domain analysis is also performed to identify any characteristic signatures, with the expectation of observing some discernible features which discriminate a sea lion from a breaking wave. As there was no independent breaking waves during the measurements (i.e. waves which were not generated by the sea lions), a Doppler spectrogram of breaking waves from a beach trial conducted in the December of 2020 is used here for comparison. The W-band data were collected from a circular polarised 94 GHz radar [10]. In Fig. 9, a spectrogram of three consecutive breaking waves is demonstrated, where the waves are receding from the radar. Diffuse distributions lasting about 2 s are observed in the Doppler signatures of the waves. For comparison, Fig. 10 (a) is a spectrogram plotted for the event when the male sea lion was commanded to jump

clear of the water, to touch a ball suspended ~3 m above the surface by a rope. The data were collected in HH polarisation here. The sea lion jumped three times causing huge splashes when landing back in the water. Very strong Doppler returns from the three splashes are clearly seen. For better visualisation, Fig. 10 (b) shows the zoomed in version, covering the 35-47s period. Here, the dispersed distribution from the water splash is seen, akin to Fig. 9 but with larger intensity, as the breaking waves in Fig. 9 are at low sea state (0 or 1). The Doppler return from the jumping sea lion is quite distinct from the breaking wave, appearing as a very narrow line due to the absence of any micro-Doppler component. This demonstrates that the Doppler information has the potential to be used for calculating statistical features for target classification training. The sinusoidal pattern is the return from the swinging ball above. It can be seen that the sinusoidal pattern increases in amplitude (increased velocity range) after the splash, from around 44 s. This is because the ball started swinging faster due to the push by the sea lion.

4 Conclusion

According to the best knowledge of the authors, this paper shows the first reported millimetre wave radar signatures of sea lions and indeed of any marine mammal. The trial was conducted in an enclosed and controlled environment, ensuring the collection of a large amount of data corresponding to the radar backscatter from the sea lions performing different activities along with their natural behaviour. The RCS of different exposed parts of the sea lions has been calculated for HH and VV polarisations. The RCS values have large variation, which is expected as they have been measured for different body parts and activities. No significant difference between the HH and VV signatures was found. It is believed that some minor discrepancies seen are mainly due the different amount of sea lion body above the water at different times. A brief Doppler analysis is also presented, mainly to point out the potential of the Doppler domain to be used for target classification feature extraction, by making a comparison with sea clutter data. For current research on sub-THz (W-band and above) radars for marine autonomous vessels, it is vital to obtain more experimental data of such animals. This will directly aid future work on automatic target recognition algorithm development.

5 Acknowledgements

This work was supported by the UK Engineering and Physical Sciences Research Council under grant EP/S032851/1. The authors acknowledge Dr Douglas Gillespie and Simon Moss from the Sea Mammal Research Unit, St Andrews, for their support with successfully organising the experimental trial. Ethical approval for the experiments was granted by the University of St Andrews Bioethics committee.

6 References

[1] D. F. Deprospo, J. Mobley, W. Hom, and M. Carron, "Radar-based Detection, Tracking and Speciation of Marine Mammals From Ships," *Areté Associates project report*, 2004.

[2] C. P. Forsyth, "Radar Detection of Marine Mammals," *Areté Associates project report*, 2010.

[3] K. Ward, R. Tough, and S. Watts, *Sea Clutter: Scattering, the K Distribution and Radar Performance*. Institution of Engineering and Technology, 2013.

[4] S. J. Anderson and J. T. Morris, "On the detection of marine mammals with ship-borne polarimetric microwave radar," in *OCEANS'10 IEEE Sydney, OCEANSSYD 2010*, 2010, pp. 1–6.

[5] D. L. McCann and P. S. Bell, "Observations and tracking of killer whales (Orcinus orca) with shore-based X-band marine radar at a marine energy test site," *Mar. Mammal Sci.*, vol. 33, no. 3, pp. 904–912, Jul. 2017.

[6] M. Mingozzi, F. Salvioli, and F. Serafino, "X-Band Radar for Cetacean Detection (Focus on Tursiops truncatus) and Preliminary Analysis of Their Behavior," *Remote Sens.*, vol. 12, no. 3, p. 388, Jan. 2020.

[7] S. Rahman and D. A. Robertson, "Coherent 24 GHz FMCW radar system for micro-Doppler studies," in *Proc. SPIE 10633, Radar Sensor Technology XXII*, 2018, no. 10633, pp. 1–9.

[8] S. Rahman and D. A. Robertson, "FAROS-E: A compact and low-cost millimeter wave surveillance radar for real time drone detection and classification," in *Proceedings International Radar Symposium*, 2021, vol. 2021-June, pp. 1–6.

[9] M. A. Richards, *Fundamentals of Radar Signal Processing*. New York: McGraw-Hill, 2005.

[10] D. A. Robertson, G. M. Brooker, and P. D. L. Beasley, "Very low-phase noise, coherent 94GHz radar for micro-Doppler and vibrometry studies," in *Proc. SPIE 9077, Radar Sensor Technology XVIII*, 2014, vol. 9077, p. 907719.